

# Anomalous thermal Hall effect and anomalous Nernst effect of CsV<sub>3</sub>Sb<sub>5</sub>

Xuebo Zhou,<sup>1,2</sup> Hongxiong Liu,<sup>2</sup> Wei Wu,<sup>2</sup> Kun Jiang,<sup>2,3</sup> Youguo Shi,<sup>2</sup>  
Zheng Li,<sup>2,3,\*</sup> Yu Sui,<sup>1,4,†</sup> Jiangping Hu,<sup>2,3</sup> and Jianlin Luo<sup>2,3,5,‡</sup>

<sup>1</sup>*School of Physics, Harbin Institute of Technology, Harbin 150001, China*

<sup>2</sup>*Beijing National Laboratory for Condensed Matter Physics and Institute of Physics,  
Chinese Academy of Sciences, Beijing 100190, China*

<sup>3</sup>*School of Physical Sciences, University of Chinese Academy of Sciences, Beijing 100190, China*

<sup>4</sup>*Laboratory for Space Environment and Physical Sciences,  
Harbin Institute of Technology, Harbin 150001, China*

<sup>5</sup>*Songshan Lake Materials Laboratory, Dongguan 523808*

(Dated: November 2, 2021)

Motivated by time reversal symmetry breaking and giant anomalous Hall effect in kagome superconductor AV<sub>3</sub>Sb<sub>5</sub> (A=Cs, K, Rb), we carried out the thermal transport measurements on CsV<sub>3</sub>Sb<sub>5</sub>. In addition to the anomalous Hall effect, the anomalous Nernst effect and the anomalous thermal Hall effect emerge. Interestingly, the longitudinal thermal conductivity  $\kappa_{xx}$  largely deviates from the electronic contribution obtained from the longitudinal conductivity  $\sigma_{xx}$  by the Wiedemann-Franz law. On the contrary, the thermal Hall conductivity  $\kappa_{xy}$  is roughly consistent with the Wiedemann-Franz law from electronic contribution. All these results indicate the large phonon contribution in the longitudinal thermal conductivity. Moreover, the thermal Hall conductivity is also slightly greater than the theoretical electronic contribution, indicating other charge neutral contributions. More than that, the Nernst coefficient and Hall resistivity show the multi-band behavior with additional contribution from Berry curvature at the low fields.

The newly discovered kagome topological metal AV<sub>3</sub>Sb<sub>5</sub> (A = K, Rb, Cs) has been found to be the first quasi-two-dimensional kagome superconductor, which becomes a new platform to investigate the interplay of topology, electron correlation effects and superconductivity [1–5]. However, whether this superconductor is unconventional owing to electron-electron correlation or conventional because of electron-phonon coupling is still under debate. From the unconventional side, both the V-shape tunneling density of states [6] and the zero-temperature residual thermal conductivity [7] have been reported. And recent low-temperature scanning tunneling microscopy (STM) resolved an unconventional pair density wave [8]. On the contrary, nuclear magnetic resonance (NMR) measurements clearly reveal the spin singlet nature and point to a conventional s-wave superconductor from the Hebel-Slichter coherence peak [9]. This nodeless property is also consistent with penetration depth measurement [10] and impurity scattering feature from STM [11]. Additionally, high resolution angle-resolved photoemission spectroscopy (ARPES) finds the weakly correlated nature of AV<sub>3</sub>Sb<sub>5</sub> and remarkable electron-phonon coupling [12].

Besides superconductivity, the charge density wave (CDW) order in this non-magnetic AV<sub>3</sub>Sb<sub>5</sub> seems to be more unconventional. Several time-reversal symmetry breaking signals have been found [13–15], especially the internal magnetic field induced relaxation rates in muon spin rotation ( $\mu$ SR) [16]. AV<sub>3</sub>Sb<sub>5</sub> also shows a giant

anomalous Hall effect (AHE), which can be attributed to the enhanced skew scattering in the CDW state and the large Berry curvature from the Kagome lattice and time-reversal symmetry breaking [17–20]. This AHE is concurrent with the CDW, indicating a strong correlation between CDW and AHE. As the thermoelectric counterpart and thermal counterpart of anomalous Hall effect, anomalous Nernst effect (ANE) and anomalous thermal Hall effect (ATHE) also play an important role in understanding quantum materials [21–24]. When the longitudinal heat flow in a magnetic field, the thermal Hall effect generates a transverse temperature gradient and the Nernst effect generates a transverse electric field, as illustrated in Fig. 1 (a). Normally, the Wiedemann-Franz (WF) law establishes a direct connection between electronic transport and electronic thermal transport [25, 26]. However, unlike the charge transport, other charge neutral excitations (e.g. phonons) can also contribute to the thermal transport. And the thermal Hall effect has been applied to probe topologically nontrivial excitations in insulators [27–29]. Hence, thermal transport provides a unique way towards identifying excitations and their topological properties.

In this work, we conducted extensive researches on the thermal transport properties of CsV<sub>3</sub>Sb<sub>5</sub>, especially the anomalous thermal Hall and the anomalous Nernst effect. Interestingly, we found that the longitudinal thermal conductivity  $\kappa_{xx}$  largely deviates the electronic thermal conductivity contribution down to 5 K. It indicates the charge neutral excitation contribution to the thermal transport. However, the thermal Hall conductivity is more or less consistent with the Hall conductivity according to WF law. Since phonons normally do not contribute to the thermal Hall,  $\kappa_{xx}$  must contain a large

\* lizheng@iphy.ac.cn

† suiyou@hit.edu.cn

‡ jlluo@iphy.ac.cn

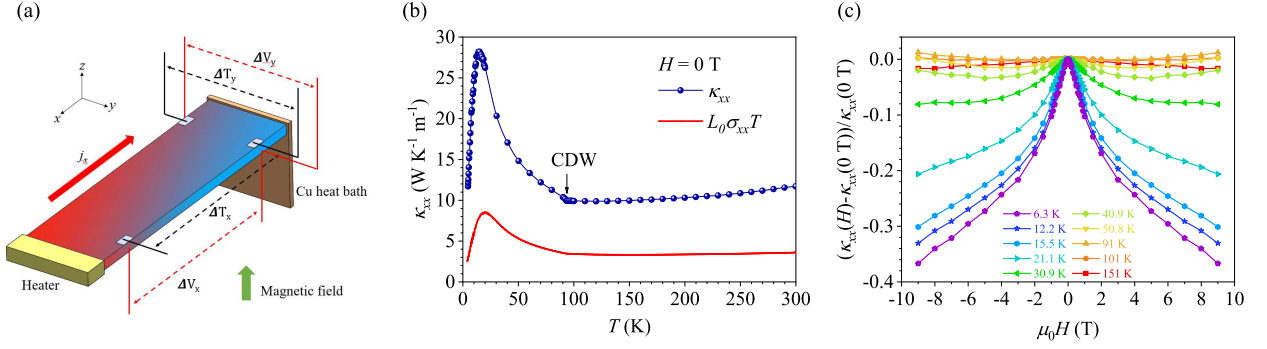


FIG. 1. (a) Schematic diagram of experimental setup. (b) Temperature dependence of longitudinal thermal conductivity  $\kappa_{xx}$ . The red curve is the electronic thermal conductivity calculated according to the WF law. Its value is smaller than the total thermal conductivity, which indicates that the phonons play an important role in thermal transportation. (c) Magnetic field dependence of longitudinal thermal conductivity  $\kappa_{xx}$ .

phonon part down to low temperature. At low temperature, the thermal Hall conductivity is still slightly higher than the theoretical value  $L_0\sigma_{xy}T$ , indicating that the thermal Hall effect may have phonon-drag mechanism or electrically neutral topological low energy excitation [30–33]. Additionally, we found the Nernst coefficient reaches a maximum value when the Hall resistivity is zero in the high magnetic field. However, this relationship no longer holds as the magnetic field decreases. Hence, the Berry curvature should also contribute to the anomalous transverse response in the low field in addition to the multi-band effect [34].

High-quality  $\text{CsV}_3\text{Sb}_5$  single crystals are prepared by a two-steps self-flux method[1]. The thermal and electrical transport measurements were performed in a 9-T Quantum Design Physical Property Measurement System. A resistance heater is used to generate a heat current. The longitudinal and transverse temperature gradients were measured with a field-calibrated chromel-AuFe<sub>0.07%</sub> thermocouples. The Nernst signal is measured by a Keithley 2182A nanovoltmeter. The sign of the Nernst coefficient can be defined in two different sign conventions. This paper is going to use the vortex convention.

The electrical conductivity tensor  $\bar{\sigma}$ , thermal conductivity tensor  $\bar{\kappa}$ , and thermoelectric conductivity tensor  $\bar{\alpha}$  relate the charge current  $\mathbf{J}_e$  and the heat current  $\mathbf{J}_q$  to the electric field  $\mathbf{E}$  and the thermal gradient  $\nabla T$  [35]:

$$\begin{pmatrix} \mathbf{J}_e \\ \mathbf{J}_q \end{pmatrix} = \begin{pmatrix} \bar{\sigma} & -\bar{\alpha} \\ T\bar{\alpha} & -\bar{\kappa} \end{pmatrix} \begin{pmatrix} \mathbf{E} \\ \nabla T \end{pmatrix} \quad (1)$$

Electrons contribute to both electrical and thermal conductivity in metals, so  $\bar{\sigma}$  relate to  $\bar{\kappa}$  by the WF law,  $\kappa_e = L_0\sigma T$ .  $\kappa_e$  is the thermal conductivity of electrons and  $L_0$  is Lorentz constant,  $L_0 \equiv \frac{\pi^2}{3} \frac{k_B^2}{e^2} = 2.44 \times 10^{-8} \text{ W}\Omega\text{K}^{-2}$ .  $\bar{\sigma}$  can be measured by applying charge current without thermal gradient ( $\nabla T = 0$ ).  $\bar{\alpha}$  and  $\bar{\kappa}$  can be measured by applying heat current without charge current ( $\mathbf{J}_e = 0$ ). Using the configuration shown in Fig. 1 (a), we measured the longitudinal thermal conductivity, the thermal

Hall conductivity, the electrical hall conductivity and the Nernst coefficient.

The temperature dependence of the longitudinal thermal conductivity  $\kappa_{xx}$  is shown in Fig. 1 (b). Above  $T_{\text{CDW}}$ ,  $\kappa_{xx}$  decreases with decreasing temperature, which is different from ordinary materials, indicating that CDW fluctuations have a strong scattering effect on electron and phonon transport. In the CDW order state, charge fluctuations are suppressed and the mean free path of electrons and phonons increase, so  $\kappa_{xx}$  increases rapidly below  $T_{\text{CDW}}$  until it reaches a peak. The total thermal conductivity is contributed by both phonons and electrons,  $\kappa = \kappa_e + \kappa_{\text{ph}}$ , where  $\kappa_e$  is the electron thermal conductivity and  $\kappa_{\text{ph}}$  is the phonon thermal conductivity. In metals with short mean free path, the thermal conductivity of phonons should be of the same magnitude as that of electrons. In order to compare the relationship between electrical conductivity and thermal conductivity, we converted electrical conductivity into electronic thermal conductivity,  $L_0\sigma_{xx}T$ , according to the WF law, as shown in Fig. 1 (b). The total thermal conductivity is greater than  $L_0\sigma_{xx}T$ . The difference is due to the phonons contribution which is of the same magnitude as the electrons contribution, indicating that phonons play an important role in the thermal transport. The magnetic field dependence of longitudinal thermal conductivity  $\kappa_{xx}$  at various temperatures is shown in Fig. 1 (c). Above 40 K, the field dependence of  $\kappa_{xx}$  is weak, while below 40 K, the field dependence of  $\kappa_{xx}$  becomes strong. The field dependence of longitudinal thermal conductivity is weaker than that of electronic conductivity, which also indicates the contribution of phonons to thermal transport.

Phonon thermal conductivity generally has no transverse effect, so the transverse thermal conductivity, namely thermal Hall conductivity, is a good method to study the thermal transport properties of electron. Figure 2 (a) and (b) shows the field dependence of electrical Hall conductivity  $\sigma_{xy}$  and thermal Hall conductivity  $\kappa_{xy}$ . Both  $\sigma_{xy}$  and  $\kappa_{xy}$  show linear field-dependent be-

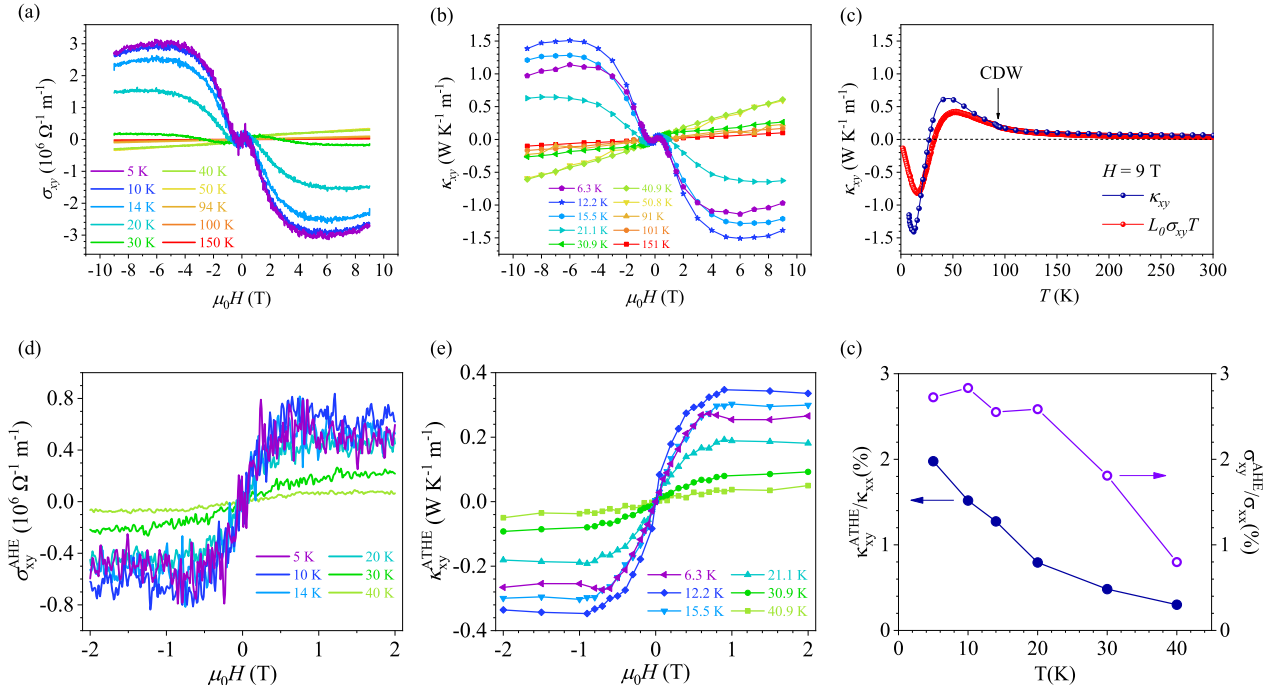


FIG. 2. (a) Magnetic field dependence of electrical Hall conductivity  $\sigma_{xy}$ . An appreciable anti-symmetric side “S” line pattern appears in the low magnetic field region below 40 K. (b) Magnetic field dependence of thermal Hall conductivity  $\kappa_{xy}$ . An anti-symmetric side “S” line pattern appears in the low magnetic field region below 40 K. (c) Temperature dependence of thermal Hall conductivity  $\kappa_{xy}$ . The red curve is the electronic thermal Hall conductivity calculated according to the WF law. (d) The extracted anomalous Hall conductivity at various temperatures. (e) The extracted anomalous thermal Hall conductivity at various temperatures. (f) Temperature dependence of anomalous thermal Hall ratio and anomalous Hall ratio.

haviors as conventional metals above  $T_{\text{CDW}}$ . Between  $T_{\text{CDW}}$  and 40 K,  $\kappa_{xy}$  is still linear magnetic field dependent in the high field region, but weak nonlinear in the low field region. Below 40 K, anomalous behaviors of thermal Hall conductivity arises. An antisymmetric edge “S” line pattern is observed in the low field region of Fig. 2 (b), which is similar to that observed in Hall coefficients. In the high field region, both the hall conductivity and the thermal Hall conductivity show saturation behaviors. We extract anomalous Hall conductivity  $\sigma_{xy}^{\text{AHE}}$  and anomalous thermal Hall conductivity  $\kappa_{xy}^{\text{AHE}}$  by subtracting a local linear ordinary electrical Hall and thermal Hall background, as shown in Fig. 2 (d) and Fig. 2 (e). The anomalous thermal Hall conductivity of CsV<sub>3</sub>Sb<sub>5</sub> reaches  $0.35 \text{ W K}^{-1} \text{m}^{-1}$ . The anomalous thermal Hall ratio is comparable to that of anomalous Hall ratio (AHR), as shown in Fig. 2 (f), which is larger than the AHR of Fe,  $\sim 0.8\%$  [36].

Figure 2 (c) shows the temperature dependence of  $\kappa_{xy}$  at 9 T. The thermal Hall effect is relatively weak at high temperature and becomes obvious with cooling. As the temperature decreases,  $\kappa_{xy}$  increases first and reaches a maximum around 40 K, which happens to be the temperature at which anomalous behaviors begin to appear. As the temperature decreases further,  $\kappa_{xy}$  changes sign at 27 K and reaches another extreme value at 12.5 K. In

order to compare the thermal Hall conductivity and the electrical Hall conductivity, we calculate the electronic thermal Hall conductivity contribution  $L_0 \sigma_{xy} T$  by using the WF law, as shown in Fig. 2 (c). The behavior of  $\kappa_{xy}$  is similar to  $L_0 \sigma_{xy} T$ , but the value is slightly larger than  $L_0 \sigma_{xy} T$ . Phonons, as neutral quasiparticles with no charge, should not directly produce thermal Hall effect. It indicates that phonon-drag mechanism or electronically neutral topological low energy excitation may exist in the thermal Hall effect of the system.

In order to further study the anomalous transverse effect, we carried out the Nernst effect measurement. The field dependence of Nernst coefficient  $N$  in CsV<sub>3</sub>Sb<sub>5</sub> at various temperatures is shown in Fig. 3 (a). Similar to Hall resistivity, the Nernst coefficient exhibits linear field-dependent behavior above  $T_{\text{CDW}}$ . When the temperature is lower than  $T_{\text{CDW}}$ , the Nernst coefficient gradually deviates from the linear magnetic field dependence and the anomalous behavior show up below 40 K.

For a single band metal, the Nernst coefficient derived from Eq. (1) is:

$$N = \frac{E_y}{\nabla_x T} = \frac{\alpha_{xy} \sigma_{xx} - \alpha_{xx} \sigma_{xy}}{\sigma_{xx}^2 + \sigma_{xy}^2} \quad (2)$$

If the electric conductivity does not depend on energy,

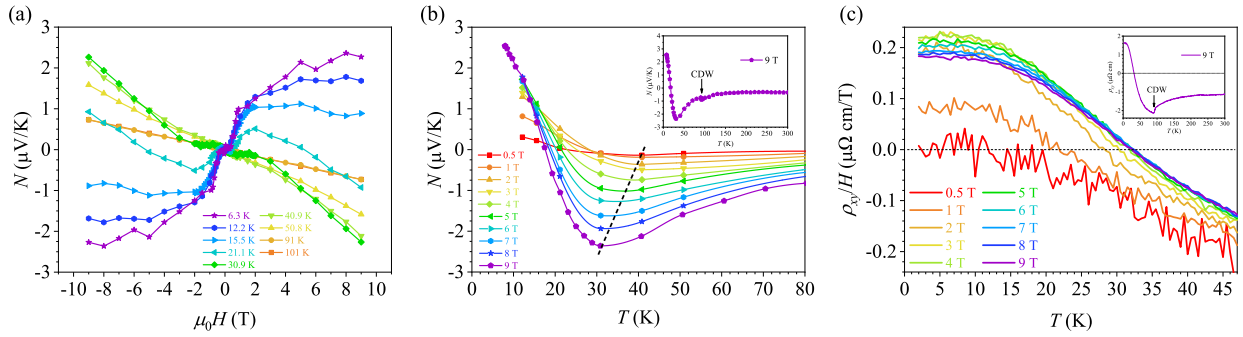


FIG. 3. (a) Magnetic field dependence of Nernst coefficient. The Nernst coefficient exhibits a linear magnetic field-dependent behavior above  $T_{\text{CDW}}$ . (b) Temperature dependence of Nernst coefficient. The Nernst coefficient shows an extreme value, which is marked by a dashed line. The temperature of the extreme value decreases as the magnetic field increases. (c) Temperature dependence of Hall resistivity divided by magnetic field. The compensation temperature of the Hall resistivity increases as the magnetic field increases.

then:

$$\frac{\sigma_{xy}}{\sigma_{xx}} = \frac{\alpha_{xy}}{\alpha_{xx}} \quad (3)$$

Therefore, the two terms in Eq. (2) are eliminated, which is called ‘‘Sondheimer cancellation’’. However, this cancellation do not affect the electrical Hall effect. On the other hand, ambipolar flow can lead to an enhancement of the Nernst signal in multi-band metals [37, 38]. Assuming two types of carriers, Eq. (2) is rewritten as:

$$N = \frac{(\alpha_{xy}^+ + \alpha_{xy}^-)(\sigma_{xx}^+ + \sigma_{xx}^-) - (\alpha_{xx}^+ + \alpha_{xx}^-)(\sigma_{xy}^+ + \sigma_{xy}^-)}{(\sigma_{xx}^+ + \sigma_{xx}^-)^2 + (\sigma_{xy}^+ + \sigma_{xy}^-)^2} \quad (4)$$

The superscripts + and – indicate the hole-like and the electron-like carriers. The  $\sigma_{xy}$  of two type carries have opposite sign, so the Sondheimer cancellation is avoid. Especially when  $\sigma_{xy}^- = -\sigma_{xy}^+$ , Eq. (4) has a maximum, which means that the Nernst coefficient will show a maximum when the Hall effect is suppressed.

The temperature variation of Nernst coefficient and Hall resistance in various magnetic fields are shown in Fig. 3 (b) and (c) respectively. At 9 T, the Nernst coefficient reaches its maximum value at 32 K where  $\rho_{xy} = 0$ , which indicates a multi-band effect. When the magnetic field decreases, the temperature of the extreme value of Nernst coefficient increases and reaches 40 K at zero field limit, while the compensation temperature of Hall resistivity decreases and approaches zero at zero field limit. Nernst and Hall signals are dominated by normal linear items in high magnetic fields, and dominated by anomalous items in low magnetic fields. Therefore, the multi-band model should not be the only reason for the relationship between Hall resistivity and Nernst coefficient in low magnetic fields. In the anomalous Hall effect studies of  $\text{AV}_3\text{Sb}_5$  [17, 18], the skew scattering has been widely pro-

posed. However, since the skew scattering does not break Sondheimer cancellation, the finite Nernst signal in low fields still has other origins, like the Berry curvature from the  $Z_2$  topological property and time-reversal symmetry breaking in  $\text{CsV}_3\text{Sb}_5$  [39, 40]. The mismatch between the thermal and electrical summations of the Berry curvature may give rise to this mismatch between Hall resistivity and Nernst coefficient [34].

In summary, we performed the thermal transport measurements on  $\text{CsV}_3\text{Sb}_5$ . Both the longitudinal thermal conductivity and the thermal Hall conductivity are larger than the theoretical values, indicating that there is a large phonon contribution in thermal transports. This shows that the phonon plays an important role in the physics of  $\text{CsV}_3\text{Sb}_5$  even at low temperature, which is consistent with the electron-phonon coupling found in ARPES [12] and a conventional s-wave superconductor from NMR [9] and penetration depth measurement [10]. The anomalous thermal Hall effect and the anomalous Nernst effect appear in the CDW state. The Nernst coefficient reaches a maximum value when the Hall resistivity is zero at 9 T, which indicates a multi-band effect. As the magnetic field decreases, the maximum of Nernst effect shifts to higher temperature, while the zero value of Hall resistivity shifts to lower temperature. It indicates that the anomalous transverse response in the low field should have a contribution from the Berry curvature.

*Note Added:* During the preparation of this manuscript, we realized that a similar anomalous Nernst effect work on  $\text{CsV}_3\text{Sb}_5$  has been posted in arXiv[41], which are consistent with our results.

This work was supported by the National Key Research and Development Program of China (Grant No. 2017YFA0302901), the National Science Foundation of China (Grant No. 12134018, 11921004, 11634015), and the Strategic Priority Research Program and Key Research Program of Frontier Sciences of the Chinese Academy of Sciences (Grant No. XDB33010100).

- [1] B. R. Ortiz, L. C. Gomes, J. R. Morey, M. Winiarski, M. Bordelon, J. S. Mangum, I. W. H. Oswald, J. A. Rodriguez-Rivera, J. R. Neilson, S. D. Wilson, E. Ertekin, T. M. McQueen, and E. S. Toberer, New kagome prototype materials: discovery of  $KV_3Sb_5$ ,  $RbV_3Sb_5$ , and  $CsV_3Sb_5$ , *Phys. Rev. Materials* **3**, 094407 (2019).
- [2] B. R. Ortiz, S. M. L. Teicher, Y. Hu, J. L. Zuo, P. M. Sarte, E. C. Schueller, A. M. M. Abeykoon, M. J. Krogstad, S. Rosenkranz, R. Osborn, R. Seshadri, L. Balents, J. He, and S. D. Wilson,  $CsV_3Sb_5$ : A  $Z_2$  Topological Kagome Metal with a Superconducting Ground State, *Phys. Rev. Lett.* **125**, 247002 (2020).
- [3] B. R. Ortiz, P. M. Sarte, E. M. Kenney, M. J. Graf, S. M. L. Teicher, R. Seshadri, and S. D. Wilson, Superconductivity in the  $Z_2$  kagome metal  $KV_3Sb_5$ , *Phys. Rev. Materials* **5**, 034801 (2021).
- [4] Q. W. Yin, Z. J. Tu, C. S. Gong, Y. Fu, S. H. Yan, and H. C. Lei, Superconductivity and Normal-State Properties of Kagome Metal  $RbV_3Sb_5$  Single Crystals, *Chinese Physics Letters* **38**, 6 (2021).
- [5] K. Jiang, T. Wu, J.-X. Yin, Z. Wang, M. Z. Hasan, S. D. Wilson, X. Chen, and J. Hu, Kagome superconductors  $AV_3Sb_5$  ( $A=K, Rb, Cs$ ) (2021), arXiv:2109.10809 [cond-mat.supr-con].
- [6] H. Zhao, H. Li, B. R. Ortiz, S. M. L. Teicher, T. Park, M. Ye, Z. Wang, L. Balents, S. D. Wilson, and I. Zeljkovic, Cascade of correlated electron states in a kagome superconductor  $CsV_3Sb_5$  (2021), arXiv:2103.03118 [cond-mat.supr-con].
- [7] C. C. Zhao, L. S. Wang, W. Xia, Q. W. Yin, J. M. Ni, Y. Y. Huang, C. P. Tu, Z. C. Tao, Z. J. Tu, C. S. Gong, H. C. Lei, Y. F. Guo, X. F. Yang, and S. Y. Li, Nodal superconductivity and superconducting domes in the topological Kagome metal  $CsV_3Sb_5$  (2021), arXiv:2102.08356 [cond-mat.supr-con].
- [8] H. Chen, H. Yang, B. Hu, Z. Zhao, J. Yuan, Y. Xing, G. Qian, Z. Huang, G. Li, Y. Ye, S. Ma, S. Ni, H. Zhang, Q. Yin, C. Gong, Z. Tu, H. Lei, H. Tan, S. Zhou, C. Shen, X. Dong, B. Yan, Z. Wang, and H.-J. Gao, Roton pair density wave in a strong-coupling kagome superconductor, *Nature* 10.1038/s41586-021-03983-5 (2021).
- [9] C. Mu, Q. Yin, Z. Tu, C. Gong, H. Lei, Z. Li, and J. Luo, S-Wave Superconductivity in Kagome Metal  $CsV_3Sb_5$  Revealed by  $^{121/123}Sb$  NQR and  $^{51}V$  NMR Measurements, *Chinese Physics Letters* **38**, 077402 (2021).
- [10] W. Duan, Z. Nie, S. Luo, F. Yu, B. R. Ortiz, L. Yin, H. Su, F. Du, A. Wang, Y. Chen, X. Lu, J. Ying, S. D. Wilson, X. Chen, Y. Song, and H. Yuan, Nodeless superconductivity in the kagome metal  $CsV_3Sb_5$ , *Science China Physics, Mechanics & Astronomy* **64**, 107462 (2021).
- [11] H.-S. Xu, Y.-J. Yan, R. Yin, W. Xia, S. Fang, Z. Chen, Y. Li, W. Yang, Y. Guo, and D.-L. Feng, Multiband Superconductivity with Sign-Preserving Order Parameter in Kagome Superconductor  $CsV_3Sb_5$ , *Phys. Rev. Lett.* **127**, 187004 (2021).
- [12] H. Luo, Q. Gao, H. Liu, Y. Gu, D. Wu, C. Yi, J. Jia, S. Wu, X. Luo, Y. Xu, L. Zhao, Q. Wang, H. Mao, G. Liu, Z. Zhu, Y. Shi, K. Jiang, J. Hu, Z. Xu, and X. J. Zhou, Electronic nature of charge density wave and electron-phonon coupling in kagome superconductor  $kv_3sb_5$  (2021), arXiv:2107.02688 [cond-mat.supr-con].
- [13] Y.-X. Jiang, J.-X. Yin, M. M. Denner, N. Shumiya, B. R. Ortiz, G. Xu, Z. Guguchia, J. He, M. S. Hossain, X. Liu, J. Ruff, L. Kautzsch, S. S. Zhang, G. Chang, I. Belopolski, Q. Zhang, T. A. Cochran, D. Multer, M. Litskevich, Z.-J. Cheng, X. P. Yang, Z. Wang, R. Thomale, T. Neupert, S. D. Wilson, and M. Z. Hasan, Unconventional chiral charge order in kagome superconductor  $KV_3Sb_5$ , *Nature Materials* **20**, 1353 (2021).
- [14] N. Shumiya, M. S. Hossain, J.-X. Yin, Y.-X. Jiang, B. R. Ortiz, H. Liu, Y. Shi, Q. Yin, H. Lei, S. S. Zhang, G. Chang, Q. Zhang, T. A. Cochran, D. Multer, M. Litskevich, Z.-J. Cheng, X. P. Yang, Z. Guguchia, S. D. Wilson, and M. Z. Hasan, Intrinsic nature of chiral charge order in the kagome superconductor  $RbV_3Sb_5$ , *Phys. Rev. B* **104**, 035131 (2021).
- [15] C. M. I. au2, D. Das, J. X. Yin, H. Liu, R. Gupta, C. N. Wang, Y. X. Jiang, M. Medarde, X. Wu, H. C. Lei, J. J. Chang, P. Dai, Q. Si, H. Miao, R. Thomale, T. Neupert, Y. Shi, R. Khasanov, M. Z. Hasan, H. Luetkens, and Z. Guguchia, Time-reversal symmetry-breaking charge order in a correlated kagome superconductor (2021), arXiv:2106.13443 [cond-mat.mtrl-sci].
- [16] L. Yu, C. Wang, Y. Zhang, M. Sander, S. Ni, Z. Lu, S. Ma, Z. Wang, Z. Zhao, H. Chen, K. Jiang, Y. Zhang, H. Yang, F. Zhou, X. Dong, S. L. Johnson, M. J. Graf, J. Hu, H.-J. Gao, and Z. Zhao, Evidence of a hidden flux phase in the topological kagome metal  $CsV_3Sb_5$  (2021), arXiv:2107.10714 [cond-mat.supr-con].
- [17] S.-Y. Yang, Y. Wang, B. R. Ortiz, D. Liu, J. Gayles, E. Derunova, R. Gonzalez-Hernandez, L. Šmejkal, Y. Chen, S. S. P. Parkin, S. D. Wilson, E. S. Toberer, T. McQueen, and M. N. Ali, Giant, unconventional anomalous Hall effect in the metallic frustrated magnet candidate,  $KV_3Sb_5$ , *Science Advances* **6**, eabb6003 (2020).
- [18] F. H. Yu, T. Wu, Z. Y. Wang, B. Lei, W. Z. Zhuo, J. J. Ying, and X. H. Chen, Concurrency of anomalous Hall effect and charge density wave in a superconducting topological kagome metal, *Phys. Rev. B* **104**, L041103 (2021).
- [19] N. Nagaosa, J. Sinova, S. Onoda, A. H. MacDonald, and N. P. Ong, Anomalous Hall effect, *Rev. Mod. Phys.* **82**, 1539 (2010).
- [20] D. Xiao, M.-C. Chang, and Q. Niu, Berry phase effects on electronic properties, *Rev. Mod. Phys.* **82**, 1959 (2010).
- [21] M. Li and G. Chen, Thermal transport for probing quantum materials, *MRS Bulletin* **45**, 348 (2020).
- [22] D. Xiao, Y. Yao, Z. Fang, and Q. Niu, Berry-phase effect in anomalous thermoelectric transport, *Phys. Rev. Lett.* **97**, 026603 (2006).
- [23] S. Onoda, N. Sugimoto, and N. Nagaosa, Quantum transport theory of anomalous electric, thermoelectric, and thermal Hall effects in ferromagnets, *Phys. Rev. B* **77**, 165103 (2008).
- [24] Y. Shiomi, Y. Onose, and Y. Tokura, Effect of scattering on intrinsic anomalous Hall effect investigated by Lorenz ratio, *Phys. Rev. B* **81**, 054414 (2010).
- [25] X. Li, L. Xu, L. Ding, J. Wang, M. Shen, X. Lu, Z. Zhu, and K. Behnia, Anomalous Nernst and Righi-Leduc Effects in  $Mn_3Sn$ : Berry Curvature and Entropy Flow,

- Phys. Rev. Lett. **119**, 056601 (2017).
- [26] L. Xu, X. Li, X. Lu, C. Collignon, H. Fu, J. Koo, B. Fauque, B. Yan, Z. Zhu, and K. Behnia, Finite-temperature violation of the anomalous transverse Wiedemann-Franz law, *Science Advances* **6**, eaaz3522 (2020).
- [27] G. Grissonnanche, A. Legros, S. Badoux, E. Lefrançois, V. Zatkó, M. Lizaire, F. Laliberte, A. Gourgout, J. S. Zhou, S. Pyon, T. Takayama, H. Takagi, S. Ono, N. Doiron-Leyraud, and L. Taillefer, Giant thermal Hall conductivity in the pseudogap phase of cuprate superconductors, *Nature* **571**, 376 (2019).
- [28] M. Hirschberger, J. W. Krizan, R. J. Cava, and N. P. Ong, Large thermal Hall conductivity of neutral spin excitations in a frustrated quantum magnet, *Science* **348**, 106 (2015).
- [29] Y. Onose, T. Ideue, H. Katsura, Y. Shiomi, N. Nagaosa, and Y. Tokura, Observation of the Magnon Hall Effect, *Science* **329**, 297 (2010).
- [30] C. Strohm, G. L. J. A. Rikken, and P. Wyder, Phenomenological Evidence for the Phonon Hall Effect, *Phys. Rev. Lett.* **95**, 155901 (2005).
- [31] L. Sheng, D. N. Sheng, and C. S. Ting, Theory of the phonon hall effect in paramagnetic dielectrics, *Phys. Rev. Lett.* **96**, 155901 (2006).
- [32] Y. Kagan and L. A. Maksimov, Anomalous hall effect for the phonon heat conductivity in paramagnetic dielectrics, *Phys. Rev. Lett.* **100**, 145902 (2008).
- [33] M. Mori, A. Spencer-Smith, O. P. Sushkov, and S. Maekawa, Origin of the phonon hall effect in rare-earth garnets, *Phys. Rev. Lett.* **113**, 265901 (2014).
- [34] L. Xu, X. Li, X. Lu, C. Collignon, H. Fu, J. Koo, B. Fauqué, B. Yan, Z. Zhu, and K. Behnia, Finite-temperature violation of the anomalous transverse Wiedemann-Franz law, *Science Advances* **6**, eaaz3522 (2020).
- [35] K. Behnia, The Nernst effect and the boundaries of the Fermi liquid picture, *J. Phys.: Condens. Matter* **21**, 9 (2009).
- [36] D. Hou, G. Su, Y. Tian, X. Jin, S. A. Yang, and Q. Niu, Multivariable Scaling for the Anomalous Hall Effect, *Phys. Rev. Lett.* **114**, 217203 (2015).
- [37] K. Behnia, The nernst effect and the boundaries of the fermi liquid picture, *Journal of Physics: Condensed Matter* **21**, 113101 (2009).
- [38] R. Bel, K. Behnia, and H. Berger, Ambipolar Nernst effect in NbSe<sub>2</sub>, *Phys. Rev. Lett.* **91**, 066602 (2003).
- [39] D. Xiao, Y. Yao, Z. Fang, and Q. Niu, Berry-phase effect in anomalous thermoelectric transport, *Phys. Rev. Lett.* **97**, 026603 (2006).
- [40] T. M. McCormick, R. C. McKay, and N. Trivedi, Semiclassical theory of anomalous transport in type-II topological Weyl semimetals, *Phys. Rev. B* **96**, 235116 (2017).
- [41] Y. Gan, W. Xia, L. Zhang, K. Yang, X. Mi, A. Wang, Y. Chai, Y. Guo, X. Zhou, and M. He, Magneto-Seebeck effect and ambipolar Nernst effect in CsV<sub>3</sub>Sb<sub>5</sub> superconductor (2021), arXiv:2110.00289 [cond-mat.supr-con].